SAND99-0094C

Multiple Input Electrode Gap Control during Vacuum Arc Remelting

C. L. Hysinger,[a] J. J. Beaman,[a] R. L. Williamson,[b] and D. K. Melgaard[b]

[a] Department of Mechanical Engineering, University of Texas, Austin, Texas 78712

[b] Sandia National Laboratories, Albuquerque, New Mexico 87185-1134

ABSTRACT

Accurate control of the electrode gap in a vacuum arc remelting (VAR) furnace has been a goal of melters for many years. The size of the electrode gap has a direct influence on ingot solidification structure. At the high melting currents (30 to 40 kA) typically used for VAR of segregation insensitive Ti and Zr alloys, process voltage is used as an indicator of electrode gap, whereas drip-short frequency (or period) is usually used at the lower currents (5 to 8 kA) employed during VAR of superalloys. Modern controllers adjust electrode position or drive velocity to maintain a voltage or drip-short frequency (or period) set-point. Because these responses are non-linear functions of electrode gap and melting current, these controllers have a limited range for which the feedback gains are valid. Models are available that relate process voltage and drip-short frequency to electrode gap. These relationships may be used to linearize the controller feedback signal. An estimate of electrode gap may then be obtained by forming a weighted sum of the independent gap estimates obtained from the voltage and drip-short signals. By using multiple independent measures to estimate the gap, a controller that is less susceptible to process disturbances can be developed. Such a controller was designed, built and tested. The tests were carried out at Allvac Corporation during VAR of 12Cr steel at intermediate current levels.

DISCLAIMER

DISCLAIMER

Portions of this document may be illegible in electronic image products. Images are produced from the best available original document.

INTRODUCTION

Vacuum arc remelting (VAR) has been used since the 1950's to produce ingots of reactive and/or segregation sensitive metal alloys.[1] In this process, a cylindrical shaped, alloy electrode is loaded into the water-cooled, copper crucible of a VAR furnace, the furnace is evacuated, and a DC arc is struck between the electrode (cathode) and some start material (e.g. metal chips) at the bottom of the crucible (anode). The arc heats both the start material and the electrode tip, eventually melting both. As the electrode tip is melted away, molten metal drips off forming an ingot beneath. Because the crucible diameter is typically 50 to 150 mm larger than the electrode diameter, the electrode must be translated downward toward the anode pool to keep the mean distance between the electrode tip and pool surface constant; this mean distance is called the electrode gap (g). As the cooling water extracts heat from the crucible wall, the molten metal next to the wall solidifies. At some distance below the molten pool surface, the alloy becomes completely solidified, yielding a fully dense ingot. After a sufficient period of time has elapsed, a quasi-steady-state situation evolves consisting of a "bowl" of molten metal situated on top of a fully solidified ingot base.[2]

There are several parameters that are important to the successful application of the VAR process and electrode gap is one of these.[3] The gap length partially regulates how the power flux is partitioned between the crucible wall and the ingot pool surface. This flux feeds the thermally and electromagnetically driven fluid flows in the pool and, thereby, directly affects the ingot solidification process. Thus, setting and maintaining the proper electrode gap is crucial for successful VAR of segregation sensitive alloys, such as nickel-based superalloys.[4] However, careful gap control is also required for high current VAR applications. Not only does it play a role in determining ingot sidewall quality, but also directly impacts the safety of the process. If the gap becomes too large and the arc attaches to the crucible wall, it may burn a hole in the crucible and allow cooling water to contact liquid titanium, potentially causing an explosion.

Normally, electrode gap is controlled by maintaining a voltage or drip-short set-point. Drip-shorts occur as molten metal drips from the electrode surface, contact the ingot pool, and momentarily extinguish the arc.[5] They have a unique electrical signature which allows them to be easily detected. The number of drip-shorts per unit time is a measure of electrode gap assuming that the melting current and furnace pressure are held constant.[6] Drip-short based electrode gap control is usually confined to relatively low current applications. This is because the drip-short frequency decreases with increasing melting current. It is typically not used for melting currents above 10 kA except in situations where it is advisable to keep the electrode tip in very close proximity to the pool surface. On the other hand, the arc voltage response to changes in electrode gap improves with increasing melting current and, for this reason, voltage is the control signal of choice for high current applications. Voltage control is usually not used when melting below 10 kA because drip-shorts are more responsive in this range.

Electrode gap control using drip-shorts or voltage is not always a straightforward proposition. VAR is also used in the production of various grades of steel, especially stainless steels or other grades that may contain alloying elements that are easily oxidized under melting conditions. Steels are usually remelted at intermediate powers with melting currents ranging from 10 to 20 kA. Often the furnace is backfilled to pressures as high as 100 to 200 Pa with argon or nitrogen to impede the escape of volatile alloying elements from the melt. This, in turn, produces intermittent glows in the furnace, a condition where the arc has transferred to the cold lateral surface of the electrode where it burns very diffusely. During a glow, the

process voltage decreases by a few volts, melting efficiency is greatly reduced, and furnace pressure climbs.[7] This presents a challenge to a voltage-based controller which interprets the decrease in voltage as a decrease in electrode gap. Because the glow disrupts melting, drip-shorts disappear, causing a drip-short based controller to interpret glow as an increase in gap.[8] Thus, an intermittent glow condition produces a processing environment that presents significant challenges to accurate control of electrode gap. Glows also occur during VAR of superalloys and titanium alloys, but only during primary melting or under anomalous process conditions. In the latter case, they are typically related to a furnace air leak or, in the case of superalloys, slag contamination.

Another difficulty encountered in electrode gap control has to do with the nonlinear relationship between gap and drip-short frequency (or period). At melting currents in the neighborhood of 6 kA, the drip-short frequency falls off very rapidly as the gap is opened from 6 to 10 mm, then flattens out and becomes unresponsive beyond about 20 mm. Accurate gap control is limited to a range of about 6 to 12 mm.[9] As melting power is increased, the fall-off occurs at smaller gaps and the range of useful operation decreases. At very high currents (30 to 40 kA), drip-shorts are only observed at very small electrode gap values (<6 mm). This nonlinear character makes it difficult to design a drip-short controller that is capable of operating over a relatively wide range of gap and current settings, especially if one desires to run at currents approaching 10 kA or at gaps beyond 10 mm.

The nonlinear character of the gap-voltage relationship is less severe. The response flattens as gap is opened but it is more highly dependent on melting current. At melting currents greater than 10 kA, the response is such as to enable relatively accurate gap control out to 50 mm and, perhaps, beyond.

In this paper, a means of electrode gap control is presented that was designed to operate over a relatively wide current range using both drip-shorts and voltage as measures of electrode gap. The controller is linear in these two control signals and, therefore, overcomes the problems associated with nonlinear control. Additionally, the controller was designed to operate under conditions where periodic glows are common and contains both a method of glow detection and a strategy for controlling through glows. The controller was developed at the Liquid Metals Processing Laboratory at Sandia National Laboratories in Albuquerque, New Mexico, and successfully implemented and tested at Allvac Corporation, Monroe, North Carolina. Testing was performed during VAR of 12-Cr steel under a nitrogen atmosphere with the process undergoing regular glows.

PROCESS CHARACTERIZATION

A factor space experiment was performed to acquire the data necessary for developing the electrode gap models. The details of this experiment are given elsewhere.[10] The factor space included melting current (8.5 to 16.9 kA), electrode gap (3 to 18 mm), and pressure (70 to 130 Pa) as the independent variables, and voltage and drip-short frequency as the dependent variables. The data were acquired during a single VAR melt in which a 0.442 m diameter electrode of 12-Cr steel weighing 4157 kg was melted into 0.533 m diameter ingot. Two trials were performed at each point in the space.

The electrode gap was determined at the beginning and end of each trial in the experiment by driving the electrode down until a dead short of at least 100 ms occurred signaling that the

electrode had contacted the molten pool surface. The distance traveled by the ram was taken as the electrode gap. Typically, a gap check required a total elapsed time of 10 s or less.

The data acquisition system was similar to that described in reference [9]. Voltage, current, pressure and ram position were continuously recorded on a Metrum Model RSR 512 digital tape system. The voltage and current signals were recorded with a 40 kHz digitization rate. Voltage was measured directly between the furnace body and the ram and divided by a factor of ten with a pure resistance voltage divider before being recorded. Current was measured with a Halmar Model 17ADM transducer. A Baratron Model 227HS pressure transducer was mounted on the furnace body and its output recorded at a 5 kHz digitization rate. Finally, ram position was measured using a mechanical encoder mounted on the furnace head.

A second data acquisition system was set up to count drip-shorts. It consisted of a PC equipped with a National Instruments MIO 16-F5 data acquisition card. The voltage signal was fed into one of the analog inputs of this card. The number of drip-shorts per second was determined and continuously logged to a data file during each trial using user-developed software.

The voltage, current and drip-short data were averaged over each of the trial periods and correlated to electrode gap. Data from those time periods during which the furnace was in a glow condition were excluded from the averaging process. The averaged data are listed in reference [10]. The following empirical models were developed from the data using standard regression techniques:

$$\hat{g}_1 = 149\, I^{-0.97} f_{DS}^{-0.42} \pm 2.5 \text{ mm} \qquad (1)$$

$$\hat{g}_2 = -101.2\frac{V}{I} - 0.25I - \frac{2304.5}{I} \pm 2.6\text{mm}. \qquad (2)$$

The residuals for these models were found to be normally distributed with zero mean, indicating that they are unbiased estimators of electrode gap.

Typically, one specifies the current at which one wishes to melt leaving the voltage, electrode gap and drip-short frequency as system variables. It is of interest to determine the noise characteristics of the measurement models as a function of melting current. The results of the analysis are shown in Table 1.

Melting Current (kA)	Variance of Voltage Model Residuals	Variance of Drip-Short Model Residuals	Covariance Between V and DS Model Residuals
8.5	12.6	11.5	10.5
13	6.5	2.4	1.3
15	3.4	5.2	4.8
17	1.2	1.2	0.8

Table 1: Noise Characteristics of the Measurement Models

CONTROLLER DESIGN

The dynamic behavior of electrode gap may be described by a relatively simple first-order differential equation, namely,

$$\dot{g} = v_{melt} - v_{ram} \tag{3}$$

where v_{melt} is the rate of change in gap due to melting and v_{ram} is the ram velocity. v_{melt} is given by

$$v_{melt} = \alpha\dot{M} + \dot{\alpha}M \tag{4}$$

where $\dot{M}$ is the melt rate, and α is a function of the liquid metal density and the electrode tip and ingot pool surface areas. The second term comes into play only if the electrode or crucible are tapered. It is now assumed that the state at time t_{i+1} may be predicted from the state at time t_i by the following standard equation from state-space control theory

$$x_{i+1} = \Phi_i x_i + \Lambda_i u_i + w_i \tag{5}$$

where x is the state vector, Φ is the state transition matrix, Λ is the input matrix, u is the input vector, and w is the process noise, assumed white. In this case, the state vector is simply the scaler, g. Making use of Equation (3), the dynamics of the system may now be described by

$$g_{i+1} = g_i + \begin{bmatrix} -1 & 1 \end{bmatrix} \begin{bmatrix} v_{ram,i} \\ v_{melt,i} \end{bmatrix} + w_i \tag{6}$$

where Φ_i=1 and Λ_i=[-1 1].

The system model described by Equation (6) presents a problem in that there is no load cell available on the VAR furnace for which the controller was being designed. With no means of estimating the melt rate and electrode mass, v_{melt} must be considered to have an infinite variance. To deal with this problem, the input matrix was set to zero and a linear observer of the system was constructed. An observer is defined as a dynamic system whose state vector is an estimate of the true state vector. The estimated state vector in this case is just the previous electrode gap estimate modified by measured values of electrode gap. The observer used to accomplish this task was a Kalman filter.

The theory of the Kalman filter will not be reviewed; it is available in most texts on state-space control theory.[11] In this approach, the dynamics of the system are given by

$$\hat{g}_{i+1} = \Phi_i \hat{g}_i + \Lambda_i u_i + K_i\left(z_i - H_i \hat{g}_i\right) \tag{7}$$

where $\hat{g}$ is the estimated electrode gap, z_i is a column vector containing its measured values, K_i is the Kalman gain matrix, and H_i is the measurement mapping matrix. In the special case considered here, Equation (7) reduces to the simple form

$$\hat{g}_{i+1} = \hat{g}_i + K_i \begin{bmatrix} z_{i,1} - \hat{g}_i \\ z_{i,2} - \hat{g}_i \end{bmatrix}. \qquad (8)$$

The term in parentheses, known as the measurement residual, is the difference between the present measured value of the electrode gap and the estimate derived from the previous estimate. Because there are no inputs in the observer, the estimate of electrode gap relies wholly on the measurements. A change in electrode gap is registered as an error in the assumption that the gap is not changing.

The Kalman gain matrix may be derived knowing the noise characteristics of the measurement model variables. The Kalman filter is an optimal linear estimator in that K_i is designed to minimize the mean square estimation error. If it is assumed that the process noise and measurement noise are uncorrelated, K_i is given by the following equation

$$K_i = P_i H^T \left[H P_i H^T + R_i \right]^{-1} \qquad (9)$$

where P_i and R_i are noise covariance matrices for the process noise and measurement noise, respectively, and the superscript T denotes the transpose of the corresponding matrix. This equation is greatly simplified in the current application. Because the state vector is a scaler, P_i has only one term. R_i, on the other hand, is a 2X2 matrix because there are two measurement models. Taking this into account, Equation (9) reduces to

$$\begin{bmatrix} K_{i,1} & K_{i,2} \end{bmatrix} = \begin{bmatrix} \frac{P_i R_{22} - P_i R_{12}}{Q_i} & \frac{P_i R_{11} - P_i R_{12}}{Q_i} \end{bmatrix} \qquad (10)$$

where Q is defined by

$$Q_i = P_i R_{22} + P_i R_{11} - 2P_i R_{12} - R_{22}^2. \qquad (11)$$

Now, because of the problem with the process model described above, P_i is taken to be infinity. Substitution of this value into Equation (10) gives the following expression

$$\begin{bmatrix} K_{i,1} & K_{i,2} \end{bmatrix} = \begin{bmatrix} \frac{R_{22} - R_{12}}{R_{11} + R_{22} - 2R_{12}} & \frac{R_{11} - R_{12}}{R_{11} + R_{22} - 2R_{12}} \end{bmatrix} \qquad (12)$$

where R_{jj} and R_{jk} are the variances and covariances listed in Table 2. If the measurement residuals for the two measurement methods were completely uncorrelated, R_{12} in Equation (12) would be zero. It is easy to see under this condition that the elements of the Kalman gain matrix reduce to terms describing the weight factors used in a weighted sum. Thus, the Kalman filter combines the measurements optimally from a statistical point of view.

The function of the controller is to form the error between the electrode gap reference set-point and the estimate of the electrode gap, and generate a control signal to drive this error to zero. The error between the reference set-point and the estimate is defined by

$$e = \hat{g} - g_{ref}. \qquad (13)$$

The type of controller used is not unique. A standard PID control algorithm has the form

$$u = K_p\left(e + T_d\frac{de}{dt} + \frac{1}{T_i}\int e\,dt\right) \qquad (14)$$

where u is the control signal, K_p is the proportional gain, T_d is the derivative time, and T_i is the integral time. In the final test of the controller, simple proportional control was used and T_d and T_i were set to zero. For this application, the control signal is the desired ram velocity.

CONTROLLER IMPLEMENTATION AND PERFORMANCE

The architecture of the controller implemented on the Allvac VAR furnace is depicted in Figure 1. All control functions shown in the figure were implemented in software on a single 486 PC. The electrode ram is driven by a hydraulic motor, the speed of which is controlled by a hydraulic servo valve. A position loop was used to control the ram through the servo valve amplifier. An absolute encoder was mounted onto the furnace head allowing for feedback of the absolute ram position. The ram position feedback was compared to a commanded position by the servo valve amplifier, which subsequently controlled the hydraulic servo valve using a proportional controller. The commanded ram position was provided by integrating the commanded ram velocity as supplied by the PID controller.

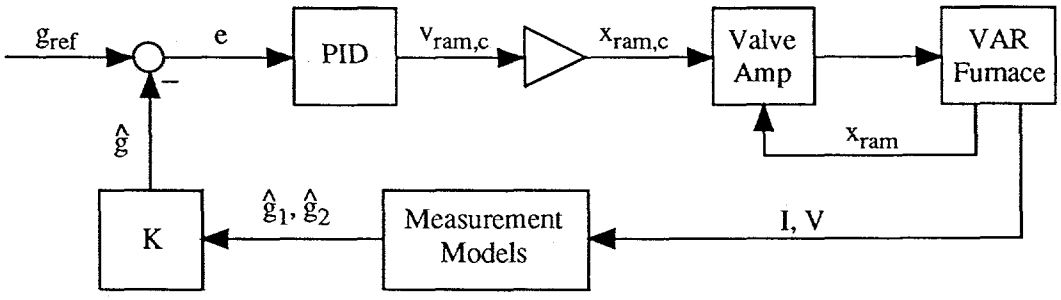

Figure 1. The layout of the control system used on the Allvac VAR furnace

In addition to the control loop shown in Figure 1, the PC was programmed to respond to process disturbances. When a glow was detected (low voltage, high pressure, no drip-shorts), the controller simply froze the ram position until the glow ceased. In this way, the gap did not change significantly during the glow. Another disturbance was characterized by large bursts of drip-shorts at relatively small electrode gaps. The PC was programmed to ignore drip-short frequencies in excess of 20 Hz and to use the previous drip-short based estimate with the present voltage based estimate.

The controller was tested during a single production melt at two different melting currents: 10.8 kA and 15.4 kA. The melt was performed under 70 Pa nitrogen. Because of severe periodic glows, the test was carried out using a relatively unresponsive proportional gain setting. Figure 2 shows a plot of the voltage trace for a portion of the melt during which the melting current was set to 15.4 kA. Note the periodic glow signature in the voltage trace indicating very unstable melting conditions.

Figures 3, 4 and 5 show average arc voltage, drip-short frequency, estimated gap and position data during three different 0.5 hour time periods. 20 s moving averages were used for all estimates. The data in Figure 3 were acquired while melting at 10.8 kA with a gap set-point of 8 mm. The data in Figures 4 and 5 were acquired at a melting current of 15.4 kA at gap set-points of 8 mm and 13 mm, respectively. One sees that the drip-shorts are relatively well behaved considering the highly unstable melt condition and that the noise in the gap estimates grows worse as the current is increased. It should be noted that the estimated gap is consistently higher than the set-point. This offset error is probably due to the unresponsive proportional gain setting and the absence of integral control action. The situation could be remedied by resetting the integral time from zero to an appropriate value.

SUMMARY AND CONCLUSIONS

A linear electrode gap controller was designed and implemented. Though the system dynamics require a measure of electrode weight, a linear observer (Kalman filter) was employed so that dynamic control could be accomplished without electrode weight data. Relatively accurate, stable electrode gap control was demonstrated under extremely unstable melting conditions during VAR of 12-Cr steel under 70 Pa nitrogen. The controller employed redundant (two) measures of electrode gap based on voltage and drip-short frequency. From a statistical point of view, this makes for more accurate control because the noise in the optimal estimate is less than the noise in either of the two independent estimates.

Because of furnace availability and test costs, the model development for this project had to be based on a single factor space experiment and the controller could only be tested during a single production melt. Obviously, such a sparse industrial development and test schedule is insufficient to optimize the controller. This was evidenced by the fact that, during the test, the voltage model was found to be less accurate than predicted by analysis of the factor space data[12] as well as by the observed offset between gap set-point and estimated gap. Despite the significant testing limitations, the controller performed well thereby demonstrating the control concept and paving the way for further development.

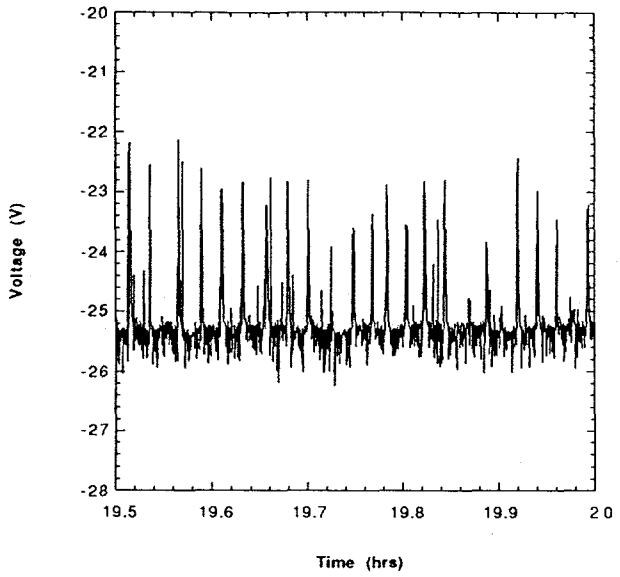

Figure 2. Typical voltage trace from the test melt showing periodic glows

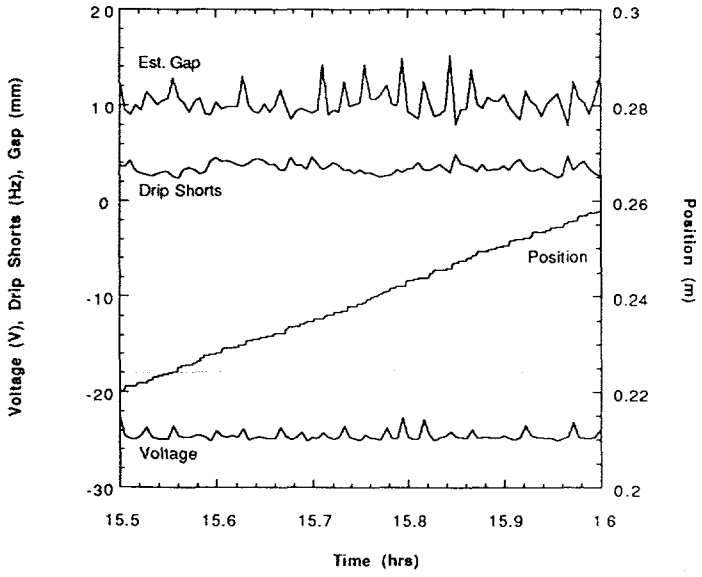

Figure 3. Controller data while melting at 10.8 kA with a gap set-point of 8 mm

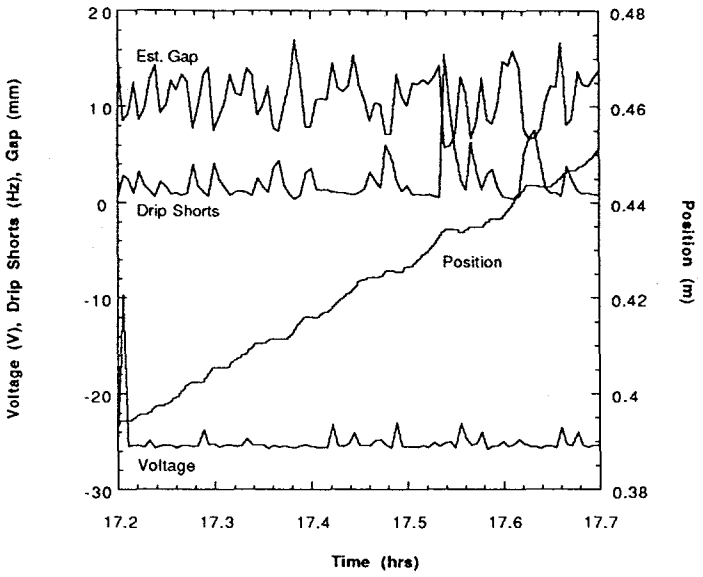

Figure 4. Controller data while melting at 15.4 kA with a gap set-point of 8 mm

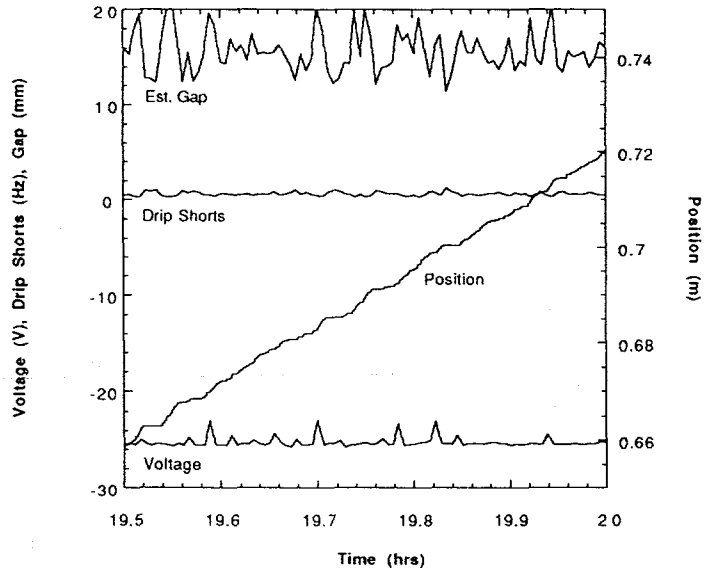

Figure 5. Controller data while melting at 15.4 kA with a gap set-point of 13 mm

ACKNOWLEDGEMENTS

A portion of this work was supported by the United States Department of Energy under Contract DE-AC04-94AL85000. Sandia is a multiprogram laboratory operated by Sandia Corporation, a Lockheed Martin Company, for the United States Department of Energy. Additional support was supplied by the Specialty Metals Processing Consortium. The authors also wish to thank Allvac Corporation, Monroe, North Carolina, for hosting the controller tests, and Charles Adasczik, then at Allvac, now at Carpenter Technology Corp., for his many contributions to making the tests possible. Thanks, also, to Greg Shelmidine for technical expertise in setting up the measurement, data collection, and control hardware.

REFERENCES

[1] For a review of vacuum arc remelting, see F.J. Zanner and L.A. Bertram, "Vacuum Arc Remelting—An Overview," *Proceedings 8th ICVM*, Interco Internationale, 1985, pp. 512-52.

[2] For high current VAR of titanium alloys, this steady-state situation is normally not reached before the end of the melt.

[3] D.K. Melgaard, R.L. Williamson, and J.J. Beaman, "Controlling Remelting Processes for Superalloys and Aerospace Ti Alloys, *JOM*, March 1998, p. 13-7.

[4] B.K. Damkroger, J.B. Kelley, M.E. Schlienger, J.A. Van Den Avyle, R.L. Williamson, and F.J. Zanner, "The Influence of VAR Processes and Parameters on White Spot Formation in Ally 718," *Proceedings of the Int'l Sym. On Superalloys 718, 625, 706 and Various Derivatives*, E.A. Loria, ed., TMS, Warrendale, Pennsylvania, 1994, pp. 125-35.

[5] F.J. Zanner, "Metal Transfer During Vacuum Consumable Arc Remelting, " *Met. Trans. B*, **10B**, 1979, pp. 133-42.

[6] F.J. Zanner, L.A. Bertram, R. Harrison, and H.D. Flanders, "Relationship between Furnace Voltage Signatures and the Operational Parameters Arc Power, Arc Current, CO Pressure, and Electrode Gap during Vacuum Arc Melting INCONEL 718," *Met. Trans. B*, **17B**, 1986, pp. 357-65.

[7] F.J. Zanner, L.A. Bertram, and R.L. Williamson, "Characterization Of Inconel 718 Alloy Metal Vapor Arc Behavior As A Function Of CO Pressure During Vacuum Arc Remelting," *Proceedings Vacuum Metallurgy Conference*, L.W. Lherbier and G.K. Bhat, ed.'s, Iron and Steel Society, Warrendale, Pennsylvania, 1986, pp. 49-54.

[8] R.L. Williamson, R. Harrison, R. Thompson, and F.J. Zanner, "The Effects Of Argon Pressurization On Melt Rate And Arc Distribution During Vacuum Arc Remelting Of Alloy 718," *Proceedings 11th International Conference on Vacuum Metallurgy*, Supplément Revue Le Vide, les Couches Minces No. 261, Mars-Avril, 1992, pp. 128-30.

[9] R.L. Williamson, F.J. Zanner, and S.M. Grose, "Arc Voltage Distribution Properties as a Function of Melting Current, Electrode Gap, and CO Pressure during Vacuum Arc Remelting," *Met. and Mat. Trans. B*, **28B**, 1997, p. 841-53.

[10] C.L. Hysinger, *The Design and Implementation of a Multiple Input Electrode Gap Controller for a Vacuum Arc Remelting Furnace*, Masters Thesis, University of Texas at Austin, Austin, Texas, December, 1995.

[11] See, for example, B. Friedland, *Control System Design: An Introduction to State-Space Methods*, McGraw-Hill, Inc., New York, NY, 1986.

[12] See reference [10] for further details.